Spectrochimica Acta Part A 74 (2009) 336–343

Contents lists available at ScienceDirect

Spectrochimica Acta Part A: Molecular and Biomolecular Spectroscopy

journal homepage: www.elsevier.com/locate/saa

Molecular interactions of monosulfonate tetraphenylporphyrin ($TPPS_1$) and meso-tetra(4-sulfonatophenyl)porphyrin (TPPS) with dimethyl methylphosphonate (DMMP)

Danqun Huo [a], Limin Yang [a], Changjun Hou [a,b,c,*], Huanbao Fa [d], Xiaogang Luo [a], Yi Lu [e,a], Xiaolin Zheng [a,b,c], Jun Yang [a], Li Yang [a,b]

[a] College of Bioengineering/Key Laboratory of Biorheology Science and Technology of Ministry of Education, Chongqing University, Shazheng Ave. 174, Chongqing 400030, PR China
[b] International Cooperation Laboratory, Chongqing University, Chongqing, PR China
[c] Key Laboratory of Micro-nano Devices and Systemic Technology of the COSTIND, Chongqing University, Chongqing, PR China
[d] College of Chemistry and Chemical Engineering, Chongqing University, Chongqing, PR China
[e] Department of Chemistry, University of Illinois at Urbana-Champaign, 600 South Mathews Avenue, Urbana, IL 61801, USA

ARTICLE INFO

Article history:
Received 4 February 2009
Received in revised form 24 May 2009
Accepted 7 June 2009

Keywords:
Porphyrins
Dimethyl methyl phosphonate
Molecular interactions
Absorbance
Fluorescence
Benesi–Hildebrand method

ABSTRACT

The molecular interactions of monosulfonate tetraphenylporphyrin ($TPPS_1$) and meso-tetra(4-sulfonatophenyl)porphyrin (TPPS) with dimethyl methylphosphonate (DMMP) have been investigated by UV–vis and fluorescence spectroscopies. The association constants and interaction stoichiometries of the bindings were obtained through Benesi–Hildebrand (B–H) method. Particularly, both linear and nonlinear fitting procedures were performed to evaluate the possible 1:2 interactions. Experimental results showed that hydrogen-bonding interactions existed in both of the two systems, resulting in regular changes in the absorbance and fluorescence characteristics of the porphyrins. The association constants and stoichiometries determined from absorbance and fluorescence studies were in excellent agreement. Using a nonlinear fitting method, we demonstrated that the one-step 1:2 interaction took place in the $TPPS_1$–DMMP system, and the association constants were determined to be 71.4 M^{-1} by absorbance measurements and 70.92 M^{-1} by fluorescence measurements. The interaction stoichiometry of the TPPS–DMMP system was 1:1, and the association constants were determined to be 16.06 M^{-1} by absorbance measurements and 16.03 M^{-1} by fluorescence measurements. It was concluded that the interaction between $TPPS_1$ and DMMP was stronger than that between TPPS and DMMP.

1. Introduction

Using chemical warfare agents (CWAs) as a weapon of terrorism has become a real existing threat. The large-scale repeated uses of nerve gases during Iran–Iraq war in the 1980s against civilians by Iraqi troops and during terrorist attacks in the 1990s by the Aum Shinrikyo sect in Japan emphasize the constant danger [1]. Since the CWAs, especially the nerve agents, are highly toxic, early alert and sensitive detection of these agents in trace level is of great importance. Accordingly, the study on detection of nerve agents has become a most active field. Due to the toxicity of the agents and usage restrictions, research on the detection of CWAs is often conducted using compounds with similar chemical structures but being non-toxic, named simulants [2]. Dimethyl methylphosphonate (DMMP) (Scheme 1) is usually used as a simulant in the lab for the detection of sarin. The research about the detection of DMMP lays a foundation for the detection of nerve agents. Such an endeavor is important for homeland security and environment monitoring.

Porphyrins are a type of macrocyclic organic molecule, which have been used for the detection of hazardous [3,4], toxic gases [5–7], environment pollutant nitro-aromatic compounds [8], insecticides and pesticides [9,10]. A porphyrin binding to another molecule will generate a complex that is likely to involve interaction with or perturbation of the extended π-bond network above and beneath the plane of the porphyrin. Since the spectrophotometric characteristics of the porphyrin are dictated by these π-orbitals, binding or interaction with another molecule is expected to alter the porphyrin spectrophotometric characteristics [11]. White and Harmon [12] demonstrated that the presence of individual organic molecules strongly affects the spectrophotometric characteristics of porphyrins.

* Corresponding author at: College of Bioengineering/Key Laboratory of Biorheology Science and Technology of Ministry of Education, Chongqing University, Shazheng Ave. 174, Chongqing 400030, PR China. Tel.: +86 23 6511 1022; fax: +86 23 6510 2507.
E-mail address: huodq@cqu.edu.cn (D. Huo).

1386-1425/$ – see front matter © 2009 Elsevier B.V. All rights reserved.
doi:10.1016/j.saa.2009.06.009

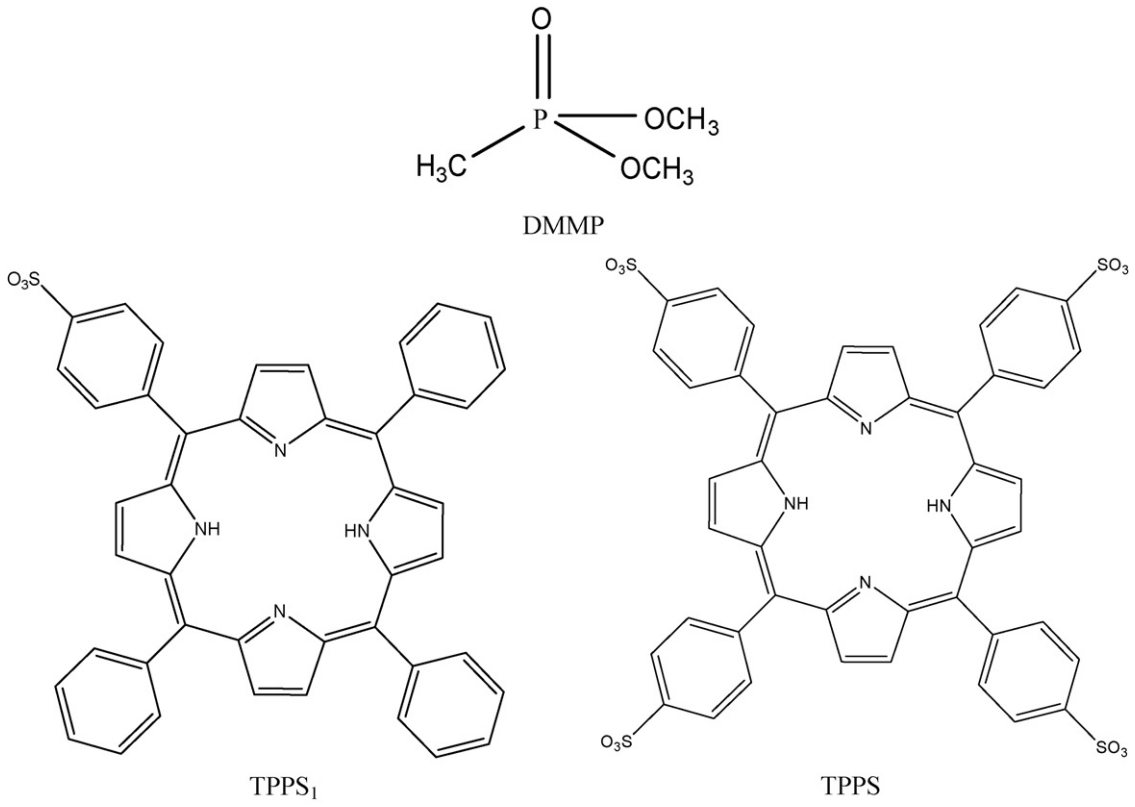

Scheme 1. Chemical structures of DMMP, $TPPS_1$ and TPPS.

Monosulfonate tetraphenylporphyrin ($TPPS_1$) and meso-tetra(4-sulfonatophenyl)porphyrin (TPPS) studied in this paper are *meso*-sulfonatophenyl substituted porphyrins, whose structural sketches are shown in Scheme 1. The two compounds have similar chemical structures, with the difference only in the number of the $-SO_3^-$ groups. Our previous reports indicate that both $TPPS_1$ and TPPS can be used to detect DMMP due to the spectral changes associated with the interactions between porphyrins and DMMP. While TPPS could detect 1000 ppm DMMP in solution, $TPPS_1$ has a superior DMMP detection sensitivity of 1 ppm. The sensitivity to DMMP is increased by 1000 times. Because of these differences in sensing performance, a detailed knowledge about the interactions of $TPPS_1$ and TPPS with DMMP is essential for understanding the mechanisms involved in the detection process. In this work, we present the results of spectroscopic study to evaluate the mechanism in DMMP detection with $TPPS_1$ or TPPS. These studies are important for the development of preventive measures against CWAs.

2. Experimental and computational method

2.1. Experimental method

2.1.1. Materials and apparatus

$TPPS_1$ and TPPS were all obtained from the Frontier Scientific (Logan, UT, USA) and used without further purification. DMMP was purchased from the Sigma (St. Louis, MO, USA). Absorbance spectra were recorded with a LAMBDA 500 spectrophotometer (CT, USA). Fluorescence spectra were measured on a RF-5301 fluorescence spectrophotometer (Shimadzu, Japan).

2.1.2. Absorbance/fluorescence measurements

If DMMP interacts with $TPPS_1$/TPPS and causes a change in the absorbance spectra, the largest change in the spectra will likely be observed in the Soret region and, for this reason, we have chosen the wavelength region from 350 to 500 nm to study the interaction of $TPPS_1$/TPPS with DMMP. Additionally, the excitation wavelength of $TPPS_1$ (414 nm)/TPPS (412 nm) was chosen in order to ensure that none of the light was absorbed by DMMP. The excitation and emission slit width was fixed at 5.0 nm. All measurements were carried out at room temperature.

A 0.2 ml of $TPPS_1$ (111.308 μM in ethanol)/TPPS (110.496 μM in deionized water) was transferred into a 10 ml volumetric flask, then different amounts of DMMP were added to yield final concentrations of 9–540 mM. The mixture was diluted to 10 ml with ethanol/deionized water and mixed thoroughly. The absorbance/fluorescence intensities were determined after letting it standing for 15 min.

2.2. Computational methods

2.2.1. Computational method for absorbance spectra

Benesi–Hildebrand (B–H) method [13] was used to determine the association constants and stoichiometries of the hydrogen bonding interactions in the porphyrin–DMMP systems. If we assume a porphyrin molecule S interacts with ligand L to form a 1:1 complex SL, that is

$$S + L \overset{K_{11}}{\longleftrightarrow} SL \tag{1}$$

then 1:1 B–H equation is as follows:

$$\frac{b}{\Delta A} = \frac{1}{S_t K_{11} \Delta\varepsilon_{11}[L]} + \frac{1}{S_t \Delta\varepsilon_{11}} \tag{2}$$

where b is the length of absorption cell ($b = 1.0$ cm), ΔA is the absorbance change during complexation; $\Delta\varepsilon_{11} = \varepsilon_{11} - \varepsilon_S - \varepsilon_L$, where ε_{11}, ε_S and ε_L are the extinction coefficient of the complex, substrate (porphyrin) and ligand (DMMP), respectively; total substrate concentration $= S_t = [S] + [SL]$ and

K_{11} = [SL]/[S][L] = association constant, where [SL] is the concentration of the complex, [S] is the concentration of the unbound substrate and [L] is the concentration of unbound ligand. In our systems L_t (total DMMP concentration) was much larger than S_t, and we can assume [L] = L_t.

By plotting $b/\Delta A$ versus 1/[L], a linear relationship can be obtained as the sufficient condition of 1:1 interaction in the stoichiometry study. The parameters can then be calculated from the intercept and slope as follows:

$$K_{11} = \frac{y - \text{intercept}}{\text{slope}} \tag{3}$$

$$\Delta\varepsilon_{11} = \frac{1}{S_t(y - \text{intercept})} \tag{4}$$

If the 1:2 interaction between porphyrin and DMMP takes place, there will be two ways. Firstly, S interacts with L gradually:

$$S + L \overset{K_1}{\longleftrightarrow} SL \tag{5}$$

$$SL + L \overset{K_2}{\longleftrightarrow} SL_2 \tag{6}$$

Then the K_1 and K_2 can be expressed as follows:

$$K_1 = \frac{[SL]}{(S_t - [SL] - [SL_2])(L_t - [SL] - 2[SL_2])} \tag{7}$$

$$K_2 = \frac{[SL_2]}{[SL](L_t - [SL] - 2[SL_2])} \tag{8}$$

But if it is a one-step interaction in the form of $S + 2L \overset{K}{\longleftrightarrow} SL_2$, then, we can obtain 1:2 B–H equation:

$$\frac{b}{\Delta A} = \frac{1}{S_t K_{11} \Delta\varepsilon_{11} [L]^2} + \frac{1}{S_t \Delta\varepsilon_{11}} \tag{9}$$

It is generally believed that the $b/\Delta A$ versus $(1/[L])^2$ plot would assure a straight line for a 1:2 complex. Thus, the 1:1 and 1:2 B–H methods can help us to obtain the association constants and stoichiometries of the interactions in porphyrin systems.

2.2.2. Computational method for fluorescence spectra

Assuming the composition of the complex is 1:1, the equation can be expressed as Eq. (10) [14]:

$$\frac{1}{F - F_0} = \frac{1}{F_1 - F_0} + \frac{1}{K[H](F_1 - F_0)} \tag{10}$$

Here F_0 and F_1 are the fluorescence intensities of the porphyrin in the absence and presence of DMMP, respectively. F is the observed fluorescence at each concentration of the porphyrin being tested. [H] is equilibrium concentration of DMMP. By plotting $1/(F - F_0)$ versus 1/[H], a linear relationship can be obtained as the sufficient condition of 1:1 interaction in the stoichiometry study. The association constant (K) can then be obtained from the ratio of the intercept to the slope, and the large association constant indicates the strong interaction between the porphyrin and DMMP.

Similar to the computational method for absorbance spectra, if it is a one-step 1:2 interaction, the equation can be expressed as Eq. (11):

$$\frac{1}{F - F_0} = \frac{1}{F_1 - F_0} + \frac{1}{K[H]^2(F_1 - F_0)} \tag{11}$$

Plotting $1/(F - F_0)$ versus $1/[H]^2$ would assure a straight line for a 1:2 complex.

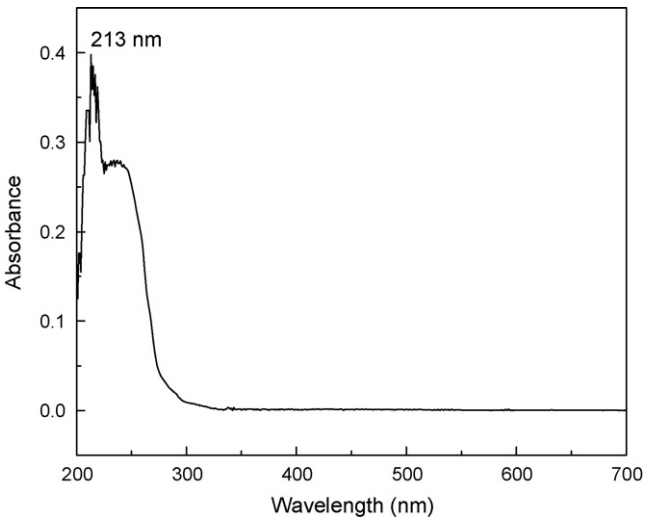

Fig. 1. DMMP in ethanol.

3. Results and discussion

3.1. Absorption spectra

3.1.1. Interaction of $TPPS_1$ and DMMP

As shown in Fig. 1, DMMP absorbs only UV light (peak at 213 nm) in ethanol. As shown in Fig. 2, the absorption spectrum of free $TPPS_1$ exhibits a typical Soret band and four Q bands. The band at 415 nm is assigned to the Soret band arising from the transition of $a_{1u}(\pi)$–$e_g^*(\pi)$, and the other four absorption maxima (512, 547, 590, and 646 nm) are attributed to the Q bands corresponding to the $a_{2u}(\pi)$–$e_g^*(\pi)$ transition [15]. The Soret band has an extinction coefficient of $1.913 \times 10^5\ M^{-1}\ cm^{-1}$ and the Q-bands have lower extinction coefficients ($\varepsilon_{512} = 1.00 \times 10^4\ M^{-1}\ cm^{-1}$, $\varepsilon_{547} = 5.1 \times 10^3\ M^{-1}\ cm^{-1}$, $\varepsilon_{590} = 3.6 \times 10^3\ M^{-1}\ cm^{-1}$ and $\varepsilon_{646} = 3.0 \times 10^3\ M^{-1}\ cm^{-1}$). These extinction coefficients have been measured using Beer's Law in our laboratory and are used for the calculation in this work.

Interaction of DMMP with $TPPS_1$ can result in the decrease in absorbance of the Soret band of $TPPS_1$ and the formation of a new absorbance band due to the binding of DMMP to $TPPS_1$. The spectral changes are more obvious in the difference spectra when we subtract the $TPPS_1$ absorbance spectrum from the $TPPS_1$ + DMMP

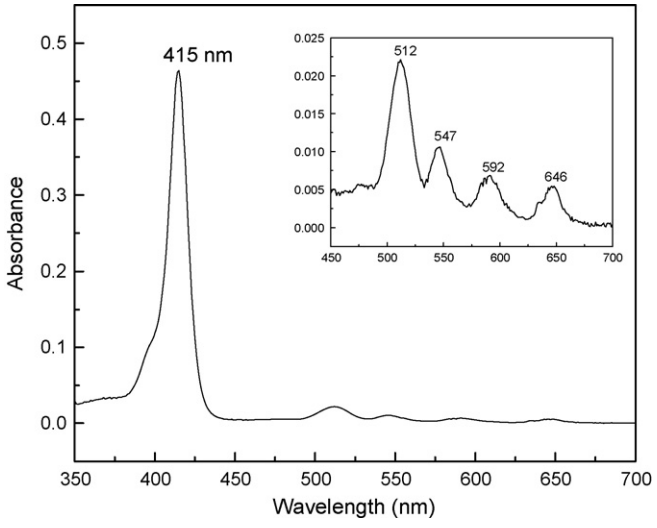

Fig. 2. $TPPS_1$ in ethanol. The inset in the upper graph shows the spectrum of Q-bands.

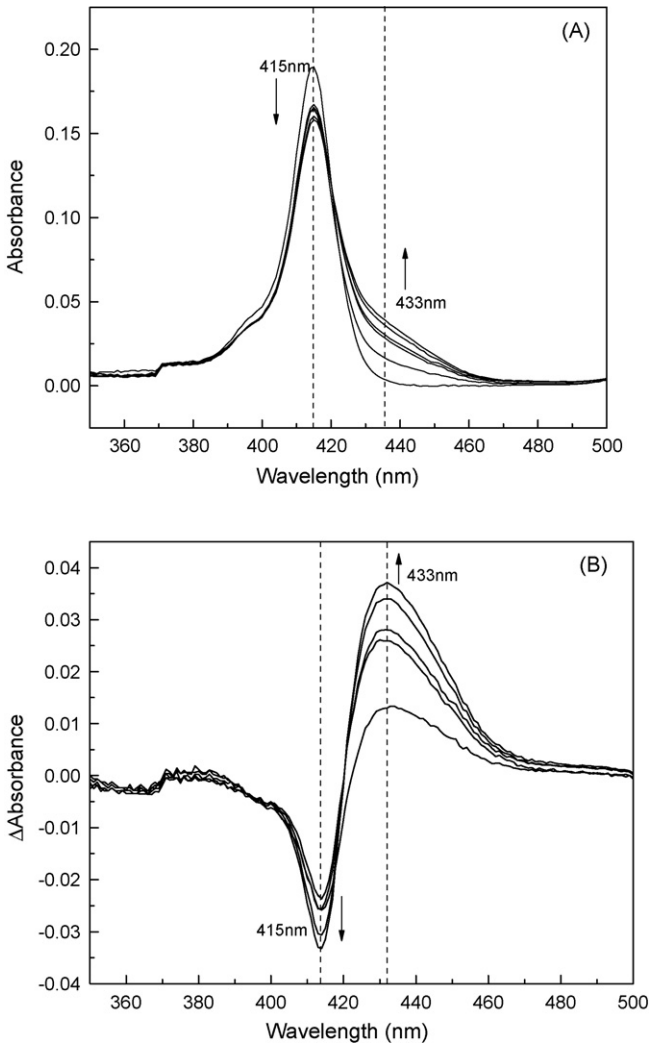

Fig. 3. (A) The absorbance spectra of $TPPS_1$ alone and $TPPS_1$ + DMMP. (B) The difference spectrum $TPPS_1$ + DMMP minus $TPPS_1$ showing a trough at 415 nm and a new peak at 433 nm. Final concentration: [$TPPS_1$] = 2.226 μM, [DMMP] = 0, 90, 180, 270, 350, and 450 mM.

absorbance spectrum (point-to-point subtraction) using UV WinLab software. Fig. 3B illustrates the difference spectra showing a trough (decrease in absorbance) at 415 nm and a peak (absorbance increase) at 433 nm. After obtaining all difference spectra for all additions of DMMP (90, 180, 270, 360, and 450 mM), we plotted the change in absorbance at 433 nm (ΔA) against the DMMP concentration and observed a hyperbolic dependence of the absorbance change at 433 nm on the DMMP concentration as shown in Fig. 4.

The 1:1 B–H method (Eq. (2)) and 1:2 B–H method (Eq. (9)) were used to investigate the association constants and stoichiometries of the interactions in the two systems. In order to satisfy the approximation condition of $[L] \approx L_t$ in the B–H method, the molar ratio of ligands to porphyrin is designed to be greater than 1000.

Presented in Fig. 5 are the 1:1 and 1:2 plots of a set of experimental data of the $TPPS_1$–DMMP system. It shows that the linear fit of 1:1 B–H plot in Fig. 5A (with a correlation coefficient R^2 of 0.9791) is less than the linear fit of 1:2 B–H plot in Fig. 5B (R^2 = 0.9912), suggesting this interaction pair is more likely in the 1:2 form. This result indicates that the interaction pattern between $TPPS_1$ and DMMP could be a one-step 1:2 interaction. The association constant (K_{11}) of the $TPPS_1$–DMMP system is calculated to be 71.4 M^{-1}, and the differential extinction coefficient ($\Delta\varepsilon_{11}$) at 433 nm is 1.71×10^4 M^{-1} cm^{-1}. Using Beer's law we calculate the

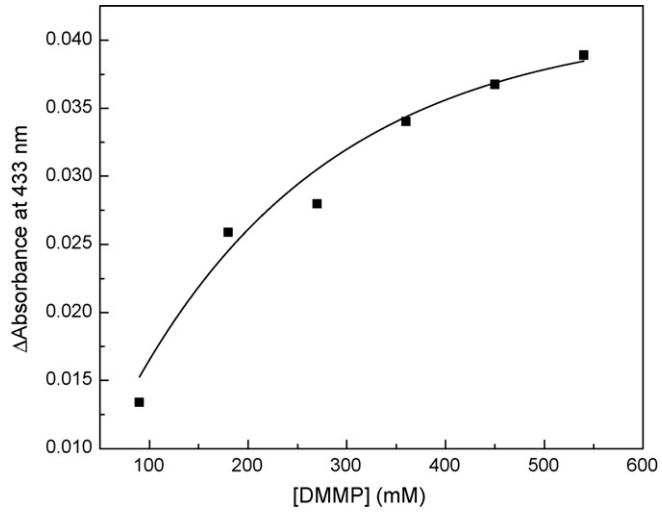

Fig. 4. Change in absorbance at 433 nm from the $TPPS_1$ + DMMP minus $TPPS_1$ versus DMMP concentration showing hyperbolic dependence on DMMP concentration.

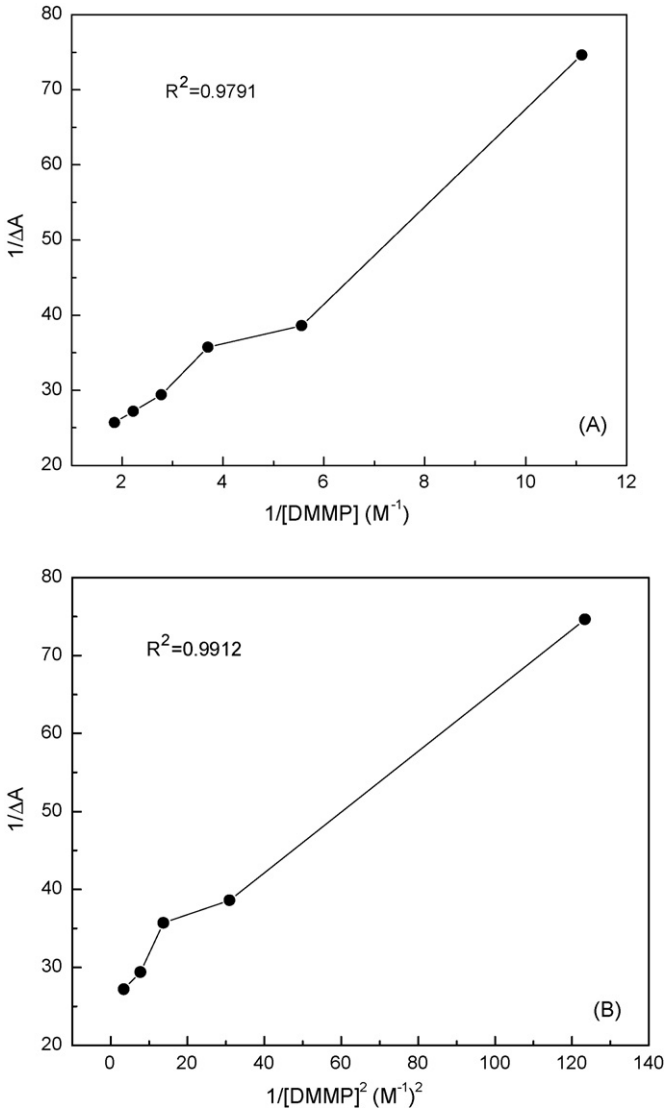

Fig. 5. 1:1 and 1:2 B–H plots at 433 nm of $TPPS_1$–DMMP system. A is the result of the 1:1 B–H plot. B is that of the 1:2 plot.

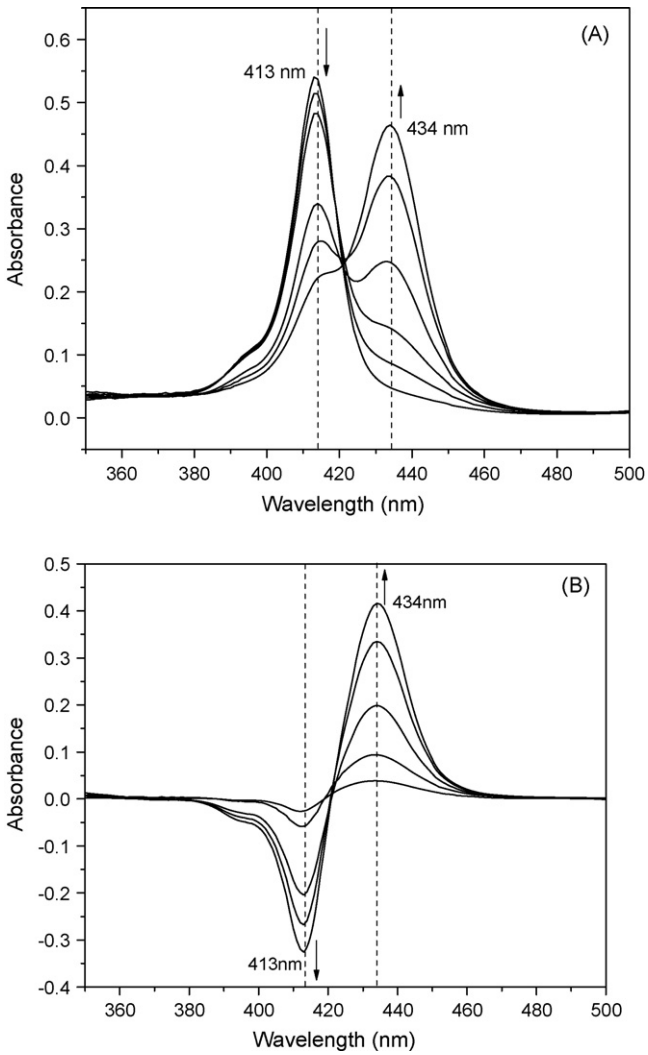

Fig. 6. (A) The absorbance spectra of TPPS alone and TPPS + DMMP. (B) The difference spectrum TPPS + DMMP minus TPPS showing a trough at 413 nm and a new peak at 434 nm. Final concentration: [TPPS] = 2.21 μM, [DMMP] = 0, 9, 18, 27, 36, and 45 mM.

extinction coefficients at 433 nm for ε_S and ε_L to be 1.02×10^4 and 0 M^{-1} cm^{-1}, respectively. Since DMMP in ethanol does not absorb at all at 433 nm, the extinction coefficient of the $TPPS_1$–2DMMP complex at 433 nm (ε_{11}) is calculated to be 2.73×10^4 M^{-1} cm^{-1}.

3.1.2. Interaction of TPPS and DMMP

Shown in Fig. 6 are the effects of different concentrations of DMMP (9–54 mM) on TPPS spectrum. Obviously, it shows that addition of DMMP to TPPS solution shifts the absorption spectrum towards higher wavelength side (red shift) accompanied by a decrease in absorbance at the Soret band (413 nm). Both red shift and decrease in absorbance at the Soret band are indicative of the binding of DMMP to TPPS. This red-shift results from TPPS working as an electron acceptor or a proton donor in the TPPS–DMMP system. Fig. 6B illustrates the difference spectra showing a trough (decrease in absorbance) at 413 nm and a peak (absorbance increase) at 434 nm when we subtract the TPPS absorbance spectrum from the TPPS + DMMP absorbance spectrum. The interaction between TPPS and DMMP can be examined in detail by using the selected UV absorption band around 434 nm. After plotting the change in absorbance at 434 nm (ΔA) against the DMMP concentration, we observed that ΔA versus DMMP concentration fitted sigmoidal-curve as shown in Fig. 7.

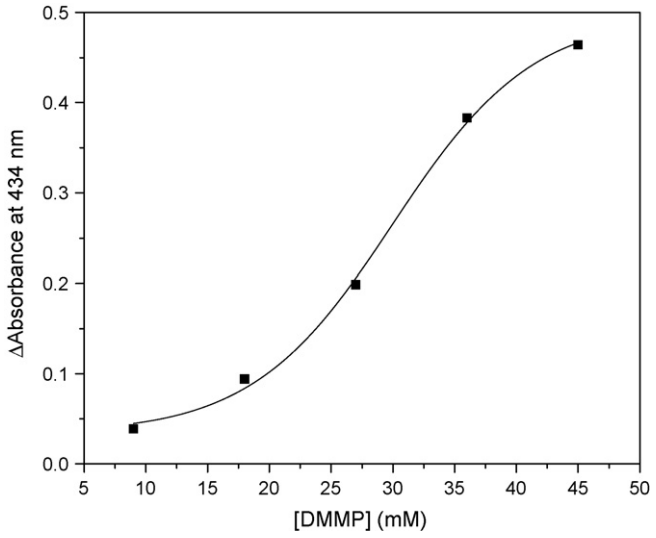

Fig. 7. Change in absorbance at 434 nm from the TPPS + DMMP minus TPPS versus DMMP concentration fitting S-curve.

The 1:1 B–H method (Eq. (2)) and 1:2 B–H method (Eq. (9)) are also used to investigate the association constants and stoichiometries of the interactions in TPPS–DMMP system. As shown in Fig. 8, the linear fit of the 1:1 B–H plot (R^2 = 0.9974) is better than that of the 1:2 B–H plot (R^2 = 0.9826) in this system. This result indicates that TPPS and DMMP interaction makes a 1:1 TPPS–DMMP complex and K_{11} = 16.06 M^{-1} and $\Delta\varepsilon_{11} = 1.08 \times 10^5$ M^{-1} cm^{-1} are obtained. The extinction coefficient of TPPS at 434 nm is 1.38×10^4 M^{-1} cm^{-1}. Again, since DMMP in deionized water does not absorb at all at 434 nm as shown in Fig. 9, the extinction coefficient of the TPPS–DMMP complex at 434 nm (ε_{11}) is calculated to be 1.218×10^5 M^{-1} cm^{-1}.

3.2. Fluorescence spectra

3.2.1. Interaction of $TPPS_1$ and DMMP

As shown in Fig. 10, $TPPS_1$ has two fluorescence emission peaks with the strong one at 648 nm and the weak one at 710 nm. At the same condition, DMMP does not show any peak at the same spectral region (550–750 nm). However, when DMMP was added into $TPPS_1$, the fluorescence intensities of $TPPS_1$ increased obviously without notable emission wavelength shifts (see Fig. 11). The change in fluorescence intensity at 648 nm ($F - F_0$) decreased as the concentration of DMMP increased. Presented in Fig. 12 are the 1:1 and 1:2 plots of the $TPPS_1$–DMMP system. It shows that 1:1 plot (R^2 = 0.97926) is less linear than 1:2 plot (R^2 = 0.99418), suggesting the interaction pair is in 1:2 form. The calculated association constant (K) obtained from the ratio of the intercept to the slope is K = 70.92 M^{-1}.

3.2.2. Interaction of TPPS and DMMP

As seen in Fig. 13, the emission of TPPS measured in water is quenched effectively by DMMP. Both red shift and decrease in fluorescence intensity at 641 nm occurs in the higher concentration of DMMP used (45 and 54 mM). Based on Fig. 13, a plot of $1/(F - F_0)$ versus 1/[H] is given in Fig. 14. The excellent linear relationship indicates the formation of a 1:1 complex (R^2 = 0.99633) between TPPS and DMMP. The calculated association constant (K) obtained from the ratio of the intercept to the slope is K = 16.03 M^{-1}. The association constants and stoichiometries determined from absorbance and fluorescence studies are in excellent agreement.

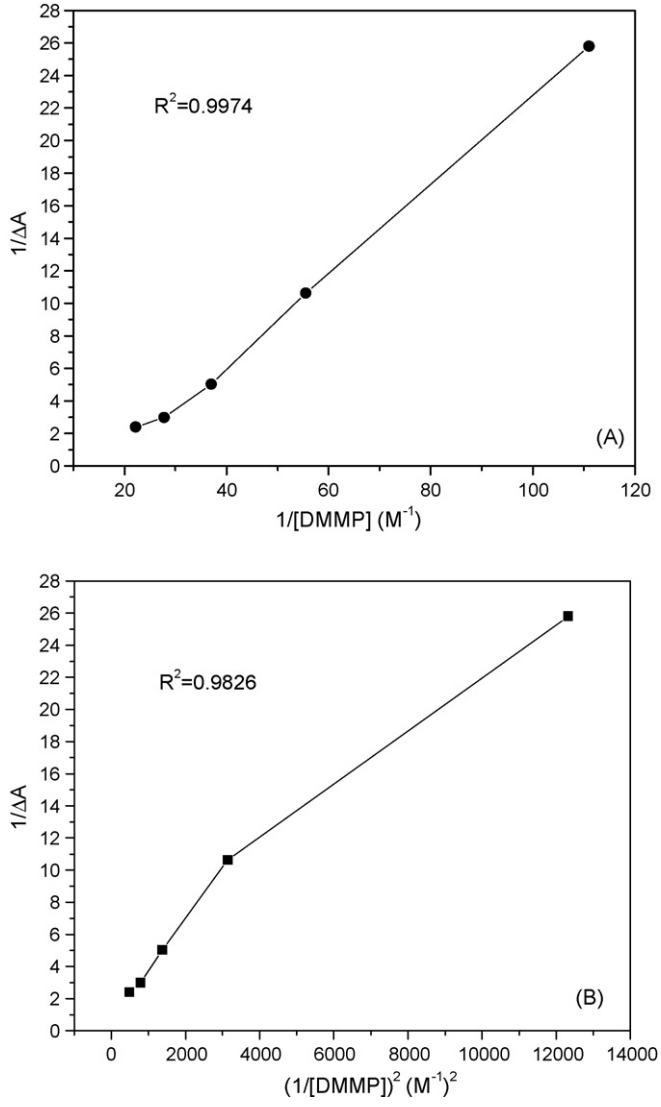

Fig. 8. 1:1 and 1:2 B–H plots at 434 nm of TPPS–DMMP system. A is the result of the 1:1 B–H plot. B is that of the 1:2 plot.

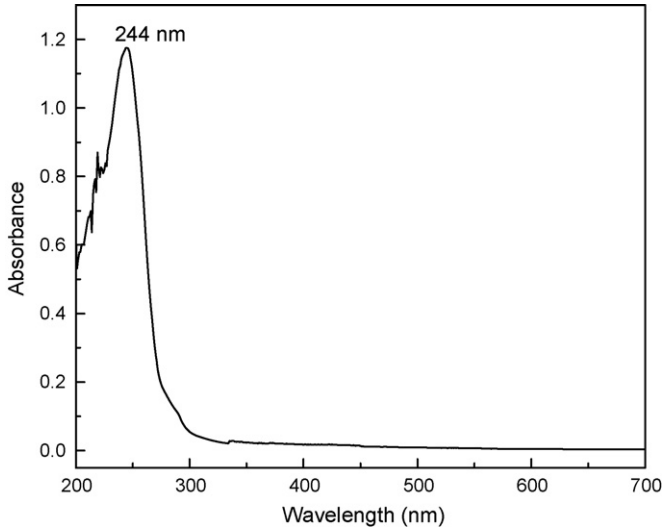

Fig. 9. DMMP in deionized water.

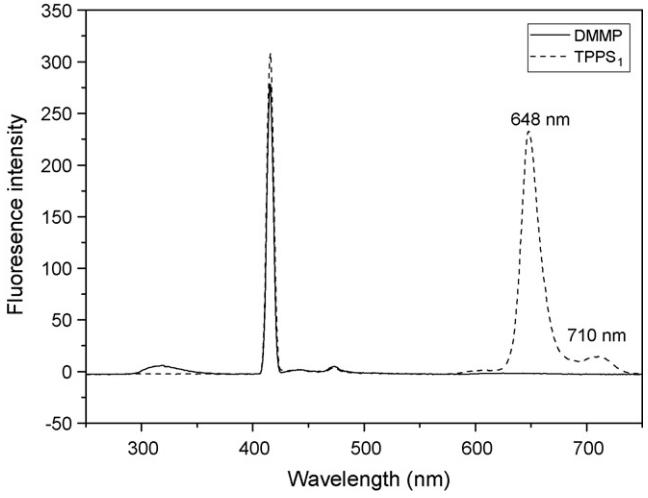

Fig. 10. Fluorescence emission spectra of $TPPS_1$ (- - -) and DMMP (—) in ethanol.

3.3. Discussion

All porphyrins have an extensive system of delocalized π electrons, which consists of four "pyrrole" units linked together by four methine bridges. Porphyrins can be modified by connecting different peripheral substitutes, changing the central metal or expanding the size of the macrocycle [16]. For instance, porphyrins that are modified with some polar groups, such as sulfonic, carboxylic, amino, or ammonium groups, become water-soluble. $TPPS_1$ and TPPS studied in this paper are *meso*-sulfonatophenyl substituted porphyrins, whose chemical structures are shown in Scheme 1.

The *meso*-sulfonation of phenyl groups not only has significant influence on phenyl groups but also alters the structure of the porphyrin macrocycle. The effects of the sulfonation on the porphyrin nucleus is considered to be the consequence of either the resonance interaction between the aromatic group and the porphyrin rings or the inductive effect of the $-SO_3^-$ groups. The resonance interaction tends to increase the electron density on the atoms of porphyrin ring, while the inductive effects can decrease the electron density of porphyrin ring due to the electron-attractive effects of the $-SO_3^-$ groups. However, the resonance interaction is less important in the case of free-base porphyrins, since the aromatic moieties are stereochemically prevented from becoming coplanar with the porphyrin

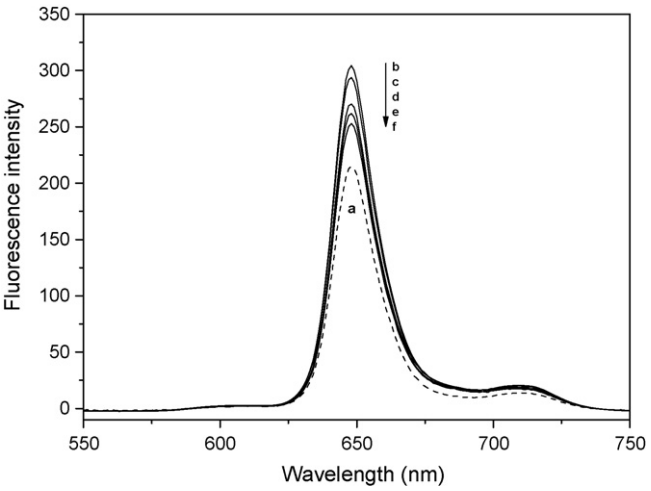

Fig. 11. Emission spectra of $TPPS_1$ (2.226 μM) at 414 nm excitation wavelength with: (a) no DMMP, (b) 135 mM, (c) 180 mM, (d) 225 mM, (e) 270 mM, and (f) 315 mM of DMMP.

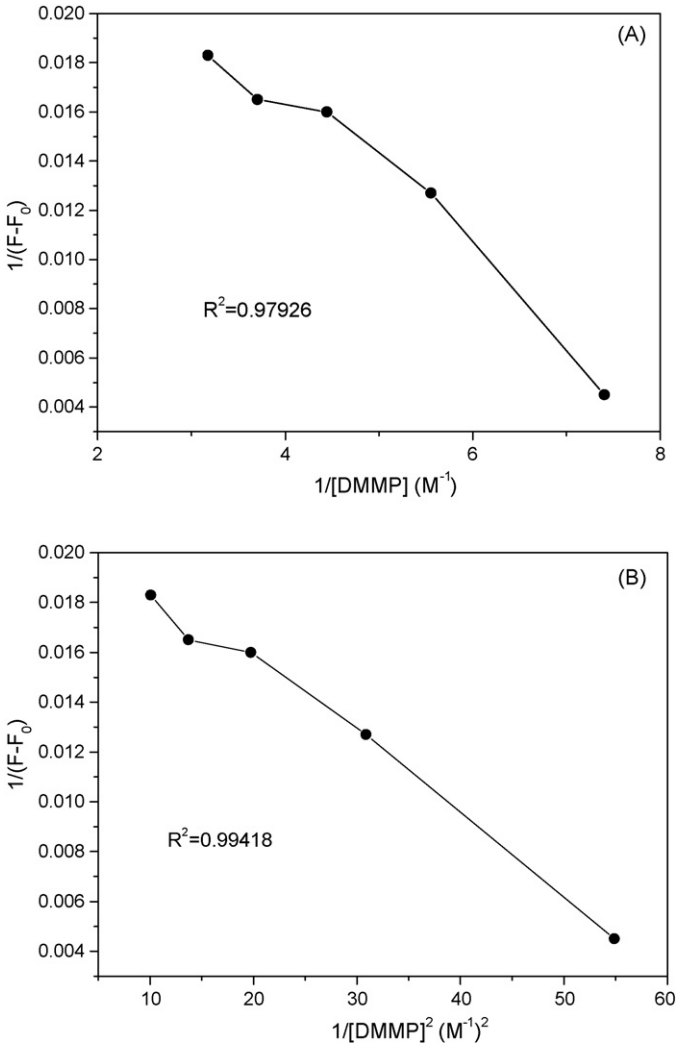

Fig. 12. 1:1 and 1:2 B–H plots at 648 nm of $TPPS_1$–DMMP system. A is the result of the 1:1 B–H plot. B is that of the 1:2 plot.

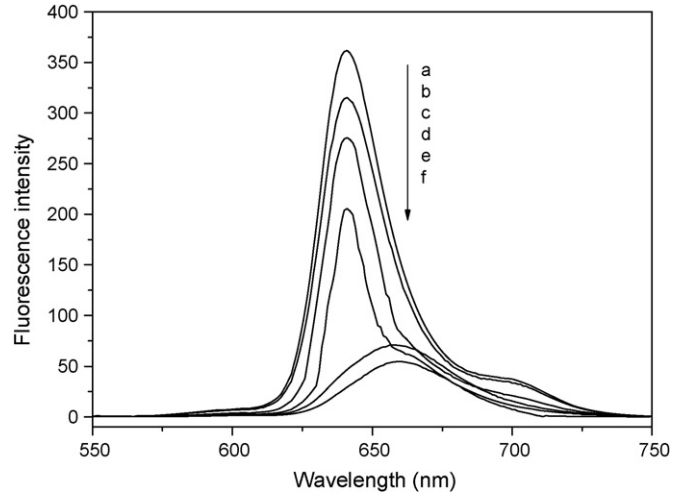

Fig. 13. Emission spectra of TPPS (2.21 μM) at 412 nm excitation wavelength with: (a) no DMMP, (b) 18 mM, (c) 27 mM, (d) 36 Mm, (e) 45 mM, and (f) 54 mM of DMMP.

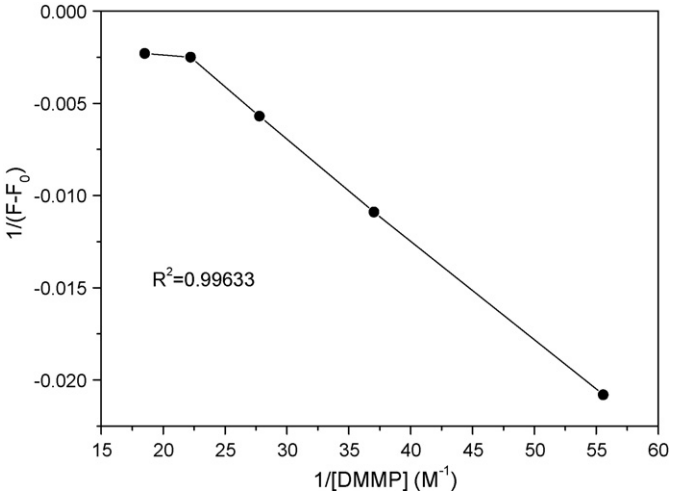

Fig. 14. 1:1 B–H plot at 641 nm of TPPS–DMMP system.

ring for TPP derivatives. Thus the inductive effect is considered to play an important role due to strong electron-withdrawing effect of the $-SO_3^-$ groups [17].

In the structure of $TPPS_1$, there is only one $-SO_3^-$ group. The electron density of porphyrin ring decreases due to the electron-withdrawing effect of the $-SO_3^-$ group. However, there is a –P═O group in the structure of DMMP, resulting in the increase of the electron density of the oxygen atom. Thus, in the $TPPS_1$–DMMP system, $TPPS_1$ acts as an electron acceptor, and DMMP acts as an electron donor. As the data demonstrates, the $TPPS_1$ interacts with two DMMP molecules. One is bound to the porphyrin through a hydrogen bond with a nitrogen atom of the central ring, while the other one is attracted by the adsorbed one. Electrons donated by DMMP make the electron distribution symmetric. As fluorescence spectra demonstrate, when DMMP was added into $TPPS_1$, the fluorescence intensities of $TPPS_1$ increased obviously.

In the TPPS–DMMP system, TPPS also acts as an electron acceptor due to the electron-withdrawing effect of the $-SO_3^-$ groups. However, four $-SO_3^-$ groups in TPPS are completely symmetrical in the stereostructure. The inductive effect of the $-SO_3^-$ groups is so weak that a TPPS interacts with only one DMMP molecule. Additionally, electrons donated by DMMP can destroy the symmetry of the electron distribution. As seen in fluorescence, DMMP quenches TPPS emission intensity.

From the molecular structure and electron distribution analysis, effects of extrinsic electrons on $TPPS_1$ and TPPS are different. Extrinsic electrons can increase the symmetry of $TPPS_1$. It is easier for the interaction between $TPPS_1$ and DMMP, and the interaction strength is also stronger. While electrons can destroy the symmetry of TPPS, and it is weaker for the interaction between TPPS and DMMP. Therefore, the sensitivity of $TPPS_1$ to DMMP is stronger than that of TPPS.

4. Conclusion

The molecular interactions of $TPPS_1$ and TPPS with DMMP have been explored by UV–vis spectroscopy. The association constants and stoichiometries determined from absorbance and fluorescence studies are in excellent agreement. The interaction stoichiometry of the TPPS–DMMP system was 1:1 according to the Benesi–Hildebrand method, and the association constants were determined to be 16.06 M^{-1} by absorbance measurements and 16.03 M^{-1} by fluorescence measurements. Using a nonlinear fitting method, we demonstrated that the $TPPS_1$–DMMP was a one-step 1:2 interaction pair, and the association constant were deter-

mined to be 71.4 M^{-1} by absorbance measurements and 70.92 M^{-1} by fluorescence measurements. The greater the association constant, the stronger the interaction between porphyrins and organic molecules. Therefore, $TPPS_1$ has higher sensitivity to DMMP than TPPS in the detection process. The $TPPS_1$'s potential ability to detect ppm level of DMMP lays a foundation for the detection of nerve agents, such as Sarin and other organophosphates. It is helpful to accomplish efficiently environmental monitoring, protect farmers, first-responders, and military personnel, and decrease the threat of chemical weapons attacks by terrorist organizations.

Acknowledgements

The authors would like to acknowledge the financial support from the National Natural Science Foundation of China (Nos. 30770568 and 30770569), the National High Technology Research and Development Program of China (863 Program) (No. 2006AA04Z349), Chongqing Municipal Natural Science Foundation and Technology Research and Development Program (No. 2008AB2024 and 2008AC7037).

References

[1] Z. Ying, Y. Jiang, X. Du, G. Xie, J. Yu, H. Wang, PVDF coated quartz crystal microbalance sensor for DMMP vapor detection, Sensor and Actuators B 125 (2007) 167–172.
[2] E. Brunol, F. Berger, M. Fromm, R. Planade, Detection of dimethyl methylphosphonate (DMMP) by tin dioxide-based gas sensor: response curve and understanding of the reactional mechanism, Sensors and Actuators B 120 (2006) (2006) 35–41.
[3] J. Andrew Legako, B.J. White, H. James Harmon, Detection of cyanide using immobilized porphyrin and myoglobin surfaces, Sensors and Actuators B 91 (2003) 128–132.
[4] Ł. Gĭorski, E. Malinowska, Fluoride-selective sensors based on polyurethane membranes doped with Zr(IV)-porphyrins, Analytica Chimica Acta 540 (2005) 159–165.
[5] K. Nakagawa, T. Aonoa, G. Uedaa, C. Tsutsumi, N. Hayase, M. Mabuchi, Y. Sadaoka, Development of an eco-friendly optical sensor element based on tetraphenylporphyrin derivatives dispersed in biodegradable polymer: effects of substituents of tetraphenylporphyrins on HCl detection and biodegradation, Sensors and Actuators B 108 (2005) 542–546.
[6] Y. Itagaki, K. Deki, S.-I. Nakashima, Y. Sadaoka, Toxic gas detection using porphyrin dispersed polymer composites, Sensors and Actuators B 108 (2005) 393–397.
[7] M. Rei Vilar, J. El-Beghadadi, F. Debontridder, R. Naaman, A. Arbel, A.M. Ferraria, A.M. Botelho Do Rego, Development of nitric oxide sensor for asthma attack prevention, Materials Science and Engineering C 26 (2006) 253–259.
[8] H. Ding, V. Erokhin, M.K. Ram, S. Paddeu, L. Valkova, C. Nicolini, A physical insight into the gas-sensing properties of copper(II) tetra-*tert*-butyl-5,10,15,20-tetraazaporphyrin Langmuir–Blodgett Films, Thin Solid Films 379 (2000) 279–286.
[9] H. Cao, J. Nam, H. James Harmon, D.H. Branson, Spectrophotometric detection of organophosphate diazinon by porphyrin solution and porphyrin-dyed cotton fabric, Dyes and Pigments 74 (2007) 176–180.
[10] A. Mufeed Awawdeh, H. James Harmon, Spectrophotometric detection of pentachlorophenol (PCP) in water using immobilized and water-soluble porphyrins, Biosensors and Bioelectronics 20 (2005) 1595–1601.
[11] M. Rahman, H. James Harmon, Absorbance change and static quenching of fluorescence of meso-tetra(4-sulfonatophenyl)porphyrin (TPPS) by trinitrotoluene (TNT), Spectrochimica Acta Part A 65 (2006) 901–906.
[12] B.J. White, H. James Harmon, Interaction of monosulfonate tetraphenyl porphyrin, a competitive inhibitor, with acetylcholinesterase, Biosensors and Bioelectronics 17 (2002) 463–469.
[13] R. Wang, Q.Z. Li, R. Wu, G.S. Wu, Z.W. Yu, Molecular interactions between pyrazine and n-propanol, chloroform, or tetrahydrofuran, Spectrochimica Acta Part A 70 (2008) 793–798.
[14] L. Wu, L. Jiao, Q. Lu, E. Hao, Y. Zhou, Spectrofluorometric studies on the interaction between oxacalix[6]arene-locked trizinc(II)porphyrins and crystal violet, Spectrochimica Acta Part A 73 (2009) 353–357.
[15] W. Zheng, N. Shan, L. Yu, X. Wang, UV–visible, fluorescence and EPR properties of porphyrins and metalloporphyrins, Dyes and Pigments 77 (2008) 153–157.
[16] E.-J. Sun, Z.-Y. Sun, M. Yuan, D. Wang, T.-S. Shi, The synthesis and properties of meso-tetra(4-alkylamidophenyl)porphyrin liquid crystals and their Zn complexes, Dyes and Pigments 81 (2009) 124–130.
[17] Y.-H. Zhang, D.-M. Chen, T. He, F.-C. Liu, Raman and infrared spectral study of meso-sulfonatophenyl substituted porphyrins ($TPPS_n$, n = 1, 2A, 2O, 3, 4), Spectrochimica Acta Part A 59 (2003) 87–101.